

Ontogeny and tissue differentiation of the pelvic girdle and hind limbs of anurans

Adriana Manzano,^{1,*} Virginia Abdala,^{2,*} María L. Ponssa^{3,*} and Mónica Soliz³

¹CONICET-UADER, Matteri y España (3105), Diamante, Entre Ríos, Argentina; ²Instituto de Herpetología, Facultad de Ciencias Naturales (UNT), Fundación Miguel Lillo-CONICET, Miguel Lillo 251 (4000), Tucumán, Argentina; ³Instituto de Herpetología, Fundación Miguel Lillo-CONICET, Miguel Lillo 251 (4000), Tucumán, Argentina

Keywords:

amphibian, development, histogenesis, skeletogenesis, appendicular skeleton

Accepted for publication:
22 May 2012

Abstract

Manzano, A., Abdala, V., Ponssa, M.L., Soliz, M. 2013. Ontogeny and tissue differentiation of the pelvic girdle and hind limbs of anurans. —*Acta Zoologica* (Stockholm) 94: 420–436.

We present the ontogeny of the integrated musculoskeletal complex that comprises the pelvic girdle and hind limbs of anurans. Our histological data show that the pelvic girdle originates from a single mesenchymatic condensation. The tissue differentiation sequence is cartilage, muscle and tendon. The intrusion of the ischiadic nerve into the limb bud is produced very early in ontogeny. The pre-cartilage appears in the pre-motile stage. Therefore, the nerve produces a movement analogous to the ‘embryonic motility’ that would induce the emergence of the pre-cartilage. The acetabulum is the first of all cavitation processes to form, the second one being the knee. The acetabulum appears before the muscles are mature, although it has been stressed that the muscle contraction maintains joint progenitors committed to their fate. Our data indicate an explosive differentiation of all 11 muscular masses together. We provide three new characters that support the monophyly of Hyloides, Acosmanura and Neobatrachia.

Adriana Manzano, CONICET-UADER, Matteri y España (3105), Diamante, Entre Ríos, Argentina. E-mail: herpetologia@gmail.com

Introduction

The pelvic girdle of anurans has been considered a conservative structure that articulates with the vertebral column by an iliosacral articulation, joining the ilial shaft with an extremely modified sacral expansion. The pelvic girdle is composed of two halves, each consisting of three bones: ischium, ilium and pubis, derived from a unique cell mass (Pomikal *et al.* 2011). The joint of these three bones forms the acetabulum, which articulates with the head of the femur (Trueb 1973; Duellman and Trueb 1986). This configuration is conserved in existing vertebrates (Jenkins and Shubin 1998) and can have different degrees of movements that have been strongly related to different modes of locomotion (Emerson 1979, 1982; Duellman and Trueb 1986; Manzano and Barg 2005; Reilly and Jørgensen 2011).

The pelvic muscular system can be divided into two groups. The first group derived from the epaxial trunk musculature and includes the muscles responsible for rotation

and sliding of the pelvis at the iliosacral articulation (Manzano and Barg 2005). The second group consists of muscles that originate on the pelvis and insert on the limb (Příkryl *et al.* 2009). Although myogenesis has been investigated in many vertebrates *in vivo* and *in vitro* (Kardon 1998), data on ontogeny of the hind limb muscles, especially in frogs, are usually restricted to one or two species of anurans (Dunlap 1967; Muntz 1975). Most of the studies are focused on *Xenopus* and *Rana* (Pomikal *et al.* 2011) and their results are extrapolated to all anurans. Intensive investigations currently address the induction of early muscle and other mesodermal tissues (Buckingham *et al.* 2003). Studies have correlated myogenesis with the development of motility, focusing on the differentiation of the muscular fibre from the myoblast (Muntz 1975). In *Xenopus laevis*, as in chicken and mice, limb muscle arises, by migration of the progenitor muscular cells of the hypaxial somite. Programmed cell death occurs during metamorphosis replacing larval muscle by an adult type muscle (Chanoine and Hardy 2003). Timing and pattern of myogenesis vary among anurans, and those differences have been correlated with life modes (Smetanick *et al.* 2000).

*All these authors contributed equally to this manuscript.

Dunlap's (1967) description of the morphogenesis of the thigh and shank muscles in *Rana pipiens* shows that the limb muscles have their origin in two major pre-muscular masses lying along the dorso-lateral and ventro-medial margins of the limb bud. Each of those masses is subsequently divided into smaller groups that will differentiate in the individual muscles.

Recently, Pomikal *et al.* (2011) described the development of the pelvic girdle in *Rana temporaria*, focusing on the relationship with the axial and appendicular system. Ročková and Roček (2005) previously addressed the ontogeny of the pelvic girdle in anurans with different locomotory types. They proposed that the basic developmental pattern is similar in all the species studied (*Discoglossus pictus*, *Bombina bombina*, *Bombina variegata*, *Bufo bufo*, *Pelobates fuscus*, *Rana dalmatina*, *X. laevis*), with only minor deviations from this pattern mainly associated with differences in water and terrestrial dwelling. Although the sample they used was clearly representative in terms of locomotory types and phylogenetic relationships, variations associated with arboreal frogs were not considered in their study. Likewise, variability in general morphology and phylogenetic history within some emblematic anuran clades, for example, hylloides (Frost *et al.* 2006), deserve further consideration.

Although ontogenetic data about skeletal elements are abundant in the literature (e.g. Fabrezi 1993; Fabrezi and Alberch 1996; Trueb *et al.* 2000; Fabrezi and Barg 2001; Maglia *et al.* 2007; Pugener and Maglia 2009), the ontogeny of the girdles and limbs, as an integrated system of skeletal elements, muscles and tendons, has been poorly investigated (e.g. Dunlap 1967; Muntz 1975; Ponssa *et al.* 2010; Pomikal *et al.* 2011).

In this study, we present the ontogeny of the skeletal complex that comprises the pelvic girdle and hind limbs of anurans, with data on the main events in the histogenesis of muscles and tendons, obtained from different species of hylloides. We also explored the origin and development of some associated structures, such as the hypochord and sacral diapophyses. Although most of our histological samples are only parts of a complete ontogeny series of each species, the comparison with data from the literature (e.g. Dunlap 1967; Ročková and Roček 2005; Ponssa *et al.* 2010; Pomikal *et al.* 2011) allows us to discuss the levels of interspecific variation in the main developmental events. The sample analysed also allowed us to discuss the evolution of some interesting ontogenetic characters in a phylogenetic context.

Materials and Methods

Clearing and staining

A total of 76 tadpoles (Stages 26–46, Gosner 1960) were used. Two to four specimens of each larval and metamorphic stages were used for the skeletal study; specimens belonged to the Hylidae family: *Phyllomedusa azurea*, *Phyllomedusa sauvagii* and *Hypsiboas riojanus* (arboreal); to the Leptodactylidae fam-

ily: *Leptodactylus latinasus* (terrestrial); and to the Leiuperidae family: *Pleurodema borellii* (terrestrial) (Appendix 1). The description of the ontogenetic pattern is based on *P. borellii*, with references to the characters that show differences in the other studied species.

The specimens were cleared and whole-mounted for double staining of cartilage and bone, following Wassersug (1976). All observations and illustrations were made using a stereo dissection microscope Carl Zeiss Discovery V8.

Histology

We completed our descriptions of skeletal ontogeny of the limbs and pelvic girdle with data on tissue differentiation in some anuran taxa, especially considering the tendon–muscle system. To obtain these data, larval specimens of Stages 26–45 (Gosner 1960) (Appendix 1) of *Scinax squalirostris* (arboreal), *Hypsiboas pulchellus* (arboreal), *P. sauvagii* (arboreal), *Pseudis minutus* (aquatic), *Dendropsophus minutus* (arboreal) and *P. borellii* (terrestrial) were processed for histological sections.

Whole larval specimens were included in Paraplast (Histoplast–Biopack Argentina) and paraffin, following the protocol for paraffin-mounting of Bancroft and Gamble (2002). Longitudinal, sagittal and transversal sections of 5–10 µm were obtained and dyed following Hematoxyline–Eosin (Bancroft and Gamble 2002) and Mallory's trichromic (modified from Totty 2002) procedures.

We follow the terminology and classification of muscles proposed by Ecker (1889), Duellman and Trueb (1986), Manzano (1996) and Prikryl *et al.* (2009); for joint development, we follow Pitsillides (2006), and for epiphyses development, Felisbino and Carvalho (1999). Identification of the pre-myogenic condensation was based on Dunlap (1967) and identification of the stages in the development of motility was according to Muntz (1975). For tissue differentiation, we considered three main stages: (i) the stage at which a pre-differentiated tissue can be observed as a tissue that is no longer mesenchymatic but still not identifiable, for example, pre-cartilage; (ii) the stage at which a particular tissue is clearly recognizable, for example, cartilage and (iii) the stage at which the tissue is completely differentiated, for example, completely mature cartilage.

Phylogenetic mapping

Fourteen characters obtained from whole-mount specimens were included in a matrix based on our observations and in the data set of Ročková and Roček (2005). Four character states were coded based on developmental stages, as conventionally recognized (Gosner 1960; Duellman and Trueb 1986): (0) early larval stages, up to Stage 37; (1) late larval stages, between stages 38–41; (2) early metamorphic stages, between stages 42–44; and (3) late metamorphic stages,

between stages 45 and 46. Characters were traced in the phylogenetic Amphibian relationship tree proposed by Frost *et al.* (2006), with the modifications proposed by Grant *et al.* (2006), and reduced to consider only the families surveyed. For optimization, we used Winclada (Nixon 1999) and obtained the tree with tree analysis using new technology (Goloboff *et al.* 2003). We follow the taxonomy proposed by Frost *et al.* (2006) and Grant *et al.* (2006).

Results

Pleurodema borellii Stages 26–32

The hind limb is composed of two small mesenchymatic buds emerging from the lateral surface of the body, which at Stage 32 are not yet chondrified.

The histological data at Stage 26 in *S. squalirostris* (Fig. 1A) show an almost circular limb bud, entirely composed of mesenchymatic cells; two streams of mesenchymatic cells can also be observed at the base of the limb bud, one on the midventral face and the other on the dorsolateral face. The streams of cells arise from the base of the tail and from the dorsal side of the abdominal region. At Stages 27–28

(Fig. 1B), nerves and mesenchymatic cell condensations can be distinguished. There is a dense gathering of mesenchymatic cells along the apical border of the limb bud. The epithelium of the limb buds is well differentiated and continuing with that of the body wall. At Stage 29 (Fig. 1C), the limb bud enlarges proximo-distally, surrounded by the epithelium, which consists in a basal membrane and two cellular layers; the compact stratum of the dermis is identified. The ischiadic nerve splits into two branches proximally, a dorsal and a ventral one. Distally, an epithelial cap is visible, covering the extreme of the developing limb, which can be interpreted as the AER region (apical ectodermal ridge). At Stage 30 (Fig. 1D), the mesenchymatic limb bud with its epithelial cover, including part of the ischiadic nerve, is evident. Three condensations of mesenchymatic cells are present, a strong condensation at the base that corresponds to the pelvic girdle, one in the middle, corresponding to the femur, and an apical one, still not identifiable. The areas of the highest cellular condensations correspond to the interzones of the future joints.

In the metapodial region of *P. sauvagii* at Stage 30 (Fig. 2A), three mesenchymatic condensations corresponding to Digit III, IV and V are visible. The peroneous nerve has already entered into the limb bud, and several

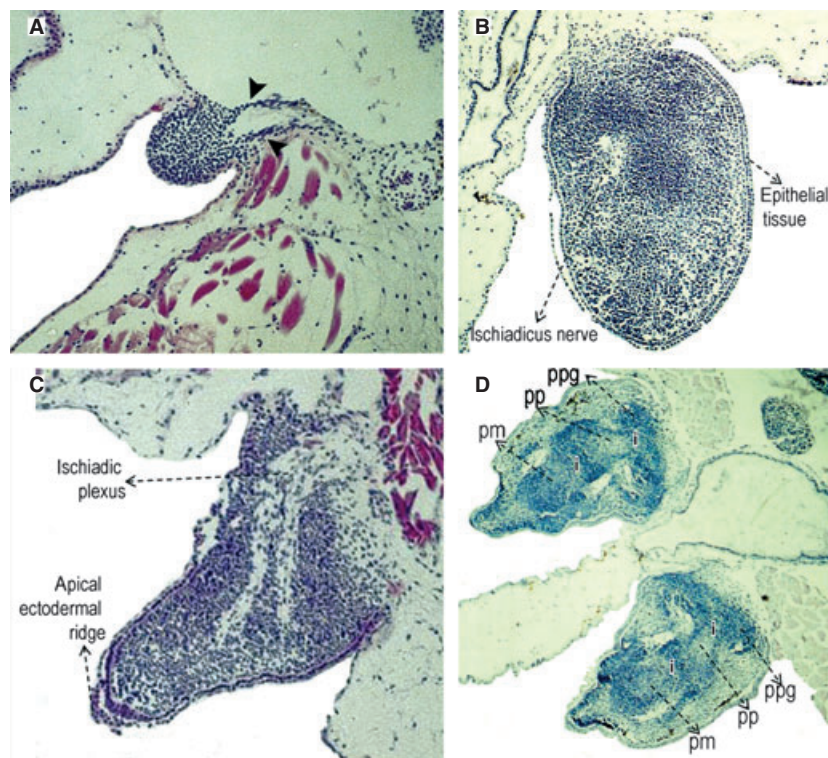


Fig. 1—**A.** Stage 26 of *Scinax squalirostris*. Limb bud entirely composed of mesenchymatic cells. Two streams of the migrating cells can be observed entering into the limb bud (black arrowhead). —**B.** Stage 27–28 of *S. squalirostris*. Limb bud entirely composed of mesenchyme. Three cell layers of epithelial tissue and the ischiadicus nerve are visible. —**C.** Stage 29 of *S. squalirostris*. Mesenchymatic limb bud with a recognizable ischiadic plexus and the apical ectodermal ridge. —**D.** Stage 30 of *S. squalirostris*. Limb bud, three mesenchymatic condensation zones signalled: the presumptive pelvic girdle, the presumptive propodium and the presumptive mesopodium. The interzones of the future joints are also visible. ppg, presumptive pelvic girdle; pp, presumptive propodium; pm, presumptive mesopodium; i, interzone.

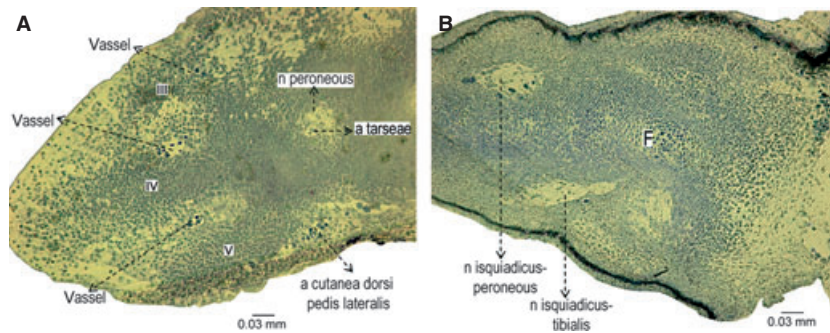


Fig. 2—**A.** Stage 30 of *Phyllomedusa sauvagii*. Histological section through limb bud where three mesenchymatic condensations corresponding to Digit III, IV and V are visible. The peroneous nerve and vessels, such as the arteria tarseae and cutanea dorsi pedis lateralis, are also observable. —**B.** Stage 31 of *Phyllomedusa sauvagii*. Histological section through limb bud where the mesenchymatic condensations corresponding to femur, tibiafibula and pre-myogenic areas are visible. The ischiadic peroneous and tibialis nerves are also distinguishable. a, arteria; F, femur; n, nerves.

vessels, such as the arteria tarseae and cutanea dorsi pedis lateralis are also visible. At Stage 31 (Fig. 2B), in the proximal region of the limb bud, mesenchymatic condensations corresponding to the femur and the tibia–fibula are visible. The ischiadic–peroneous and ischiadic–tibialis nerves are present.

Pleurodema borellii Stage 33–34

The ischium/pubis, femur, tibia–fibula, tarsals, metatarsals and one phalanx of the Toe IV are visible and cartilaginous. The hypochord is cartilaginous.

The histological data of Stage 33 on *H. pulchellus* (Fig. 3A) show that the pelvic girdle condensation remains unchanged as in Stage 30 of *Scinax squatrostris*. Two chondrogenic foci previously described in those species are present along the limb, one on the femur and a smaller one on the area corresponding to the presumptive tibia–fibula. The limb is lengthening proximo–distally. On the surface of the skeletal elements, there are four large mesenchymal condensations, which may be identified as future muscular masses. Two of them are continuous proximally with the mesenchyme of the developing pelvic girdle and pelvic–femur joint and distally with the mesenchyme of the developing knee joint. Another one is located ventro–medially and extends from the developing knee joint to the developing ankle. The fourth one is the most superficial; it extends covering the ventro–medial layer already described. Stage 34 of *S. squatrostris* (Fig. 3B) shows evidence of the developing pelvic girdle with three foci of chondrogenic cells present. The acetabulum is visible and clear. At the central areas of each presumptive bone, mature hypertrophic chondrocytes with abundant extracellular matrix (ECM) are present. At this ontogenetic stage, the presumptive femur shaft forms an obtuse angle with the sagittal plane of the body. At least 11 pre-myogenic foci are distinguishable at the three segments of the limb. However, at the level of the pelvic, knee and ankle regions, the developing muscles end into a dense condensation of mesenchymatic cells. One of the 11

foci is a large pre-myogenic condensation of cells that lies dorsal and parallel to the thigh and into which the ischiadic nerve penetrates. This pre-myogenic condensation corresponds to the anlagen of the gluteus magnus–cruralis muscular complex. A second focus is continuous with the anterior pre-myogenic complex and extends proximally, bordering the outer edge of the pelvic girdle condensation, and ventrally, entering the undifferentiated mesenchymatic condensation at the pelvic–femur joint. This pre-myogenic complex corresponds to the anlagen of the iliacus–pectineus muscular complex. There is another group of cells corresponding to the anlagen of the tensor fasciae latae–cruralis muscular complex that are continuous with the gluteus magnus–cruralis complex. At the same time, a longitudinally oriented mass of cells, which lies parallel to, but independent of, the gluteus magnus, distally enters the mesenchyme of the knee joint. It corresponds to the anlagen of the gluteus magnus.

A ventro–medial pre-myogenic mass of cells can also be distinguished, contacting proximally with an undifferentiated group of mesenchymatic cells from the pelvic–femur joint and with the region of the knee joint. This mass of cells distally contacts with the undifferentiated mesenchyme of cells of the tibia–fibula. It can be subdivided into a proximo–lateral mass of cells, broadly in contact with the mesenchyme of the pelvis and the pelvic–femur joint, which corresponds to the anlagen of the gemellus muscle. The other division is ventral and corresponds to the anlagen of the semimembranosus–adductor muscular complex.

Dorsolaterally, an independent mesenchymatic condensation can be distinguished close to the developing tibia–fibula. This condensation probably corresponds to the primordium of the dorsal surface of the shank and of the tarsal muscles, such as the peroneous–tibialis anticus longus. At the ventral surface, two mesenchymatic areas are distinguishable: one is surrounding the femur–tibia–fibula joint and corresponds to the presumptive tibialis posticus muscle; the other is surrounding the tibia–fibula tibiale–fibulare joint (‘ankle joint’) and corresponds to the presumptive plantaris longus muscle.

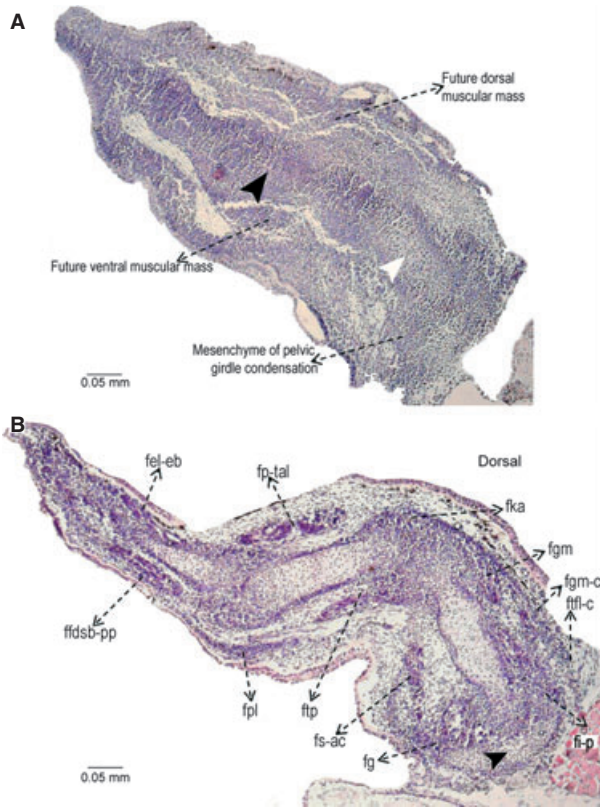


Fig. 3—**A.** Stage 33 of *Hysiboa pulchellus*. Histological section through mesenchymal condensation of the future pelvic girdle and hind limb. Chondrogenic foci are present in sections through the propodial (white arrowhead) and metapodial (black arrowhead) segments. Mesenchymal condensation can be identified as the future dorsal and ventral myogenic masses. —**B.** Stage 34 of *Scinax squalirostris*. Histological sections through hind limb and pelvic girdle. The chondrogenic foci of the pelvic girdle are visible (black arrowhead). Eleven myogenic foci are distinguishable in the segments of the limb. fel-eb, future extensor longus–extensores brevis muscular complex; ffdsb-pp, future flexor digiti superficialis brevis–plantaris profundus muscular complex; fg, future gemellus muscle; fgm, future gluteus magnus muscle; fgm-c, future gluteus magnus–cruralis muscular complex; fi-p, future iliacus–pectineus muscular complex; fka, future knee aponeurosis; fpl, future plantaris longus muscle; fp-tal, future peroneus–tibialis anticus longus muscular complex; fs-ac, future semi-membranosus–adductor muscular complex; ftfl-c, future tensor faciae latae–cruralis muscular complex; ftp, future tibialis posticus muscle.

In the most distal part of the hind limb, at the dorsal surface, another mesenchymatic condensation is distinguishable, although not clearly separated from that of the skeletogenous tissue. This condensation corresponds to the presumptive extensor longus and extensores brevis complexes. Ventral to the previously described condensation, there is another mesenchymatic group of cells that corresponds to the anlagen of the flexor digiti superficialis brevis–plantaris profundus muscular complex.

Pleurodema borellii Stage 35

The plate corresponding to the ischium/pubis is distinguishable and cartilaginous (Fig. 4A). The pelvic girdles are separated. The ilium is located in a vertical position related to the vertebral column; this element is posterior to the first post-sacral element. The long bones of the meso and metapodium are visible and their central areas

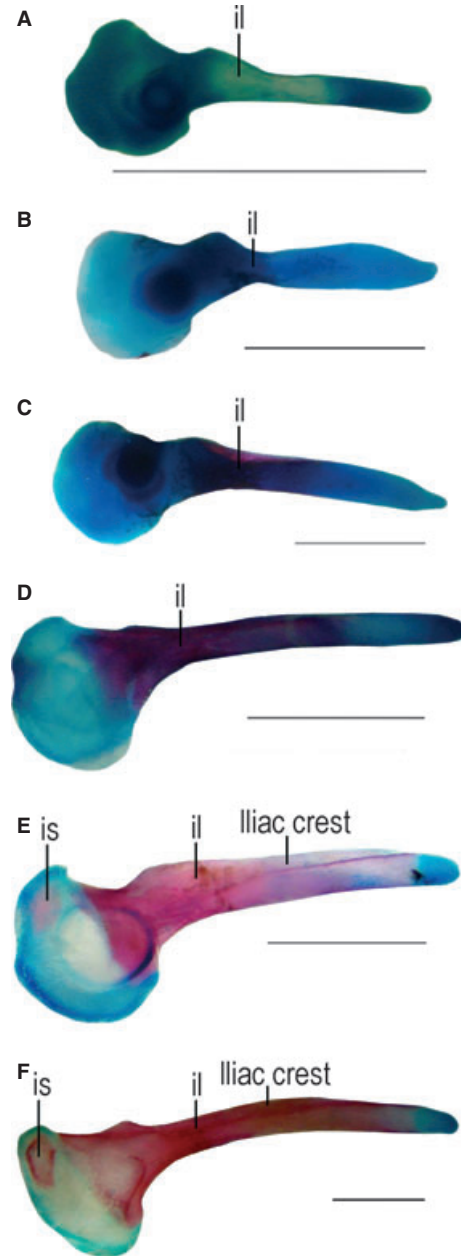


Fig 4—*Pleurodema borellii*. Developmental series of a diaphanized pelvic girdle. —**A.** Stage 36. —**B.** Stage 38. —**C.** Stage 40. —**D.** Stage 42. —**E.** Stage 44. —**F.** Stage 46. il, ilium; is, ischium. Scale bar: 1 mm.

are well stained. The femur is oriented to the posterior region of the body. In the autopodium, small spots corresponding to the cartilaginous metatarsus and to the phalanx of Toe IV are present (Fig. 5A). The ossification of the hypochord starts to be distinguishable.

The histological data of *S. squalirostris* at this stage (Fig. 6A) show that the epithelial tissue has four cell layers. The most superficial cells are flat, each with its nucleus located parallel to the tissue surface. The cells of the middle stratum have rounded nuclei, whereas in the deeper layer, cells are located closer to one another and have oval nuclei. The developing pelvic girdle remains unchanged. The acetabulum is more delimited than at the previous stage. The proximal epiphysis of the femur is distinguishable as a mesenchymatic condensation; the chondrogenic foci corresponding to the presumptive lateral articular cartilages are also present. The distal epiphysis of the femur is still undifferentiated, and the interzone remains visible in the area of the future femur–tibia–fibula joint.

Continuous with the anterior and posterior extremes of the developing pelvic girdle, two pre-myogenic zones can be identified; in both zones, three defined but broadly interconnected parts can be recognized. One additional large, ventromedial mass of pre-myogenic tissue can be also recognized. This is in contact proximally with the mesenchyme of the pelvic girdle and distally with the knee joint and the tibia–fibula mesenchyme.

In *P. minutus* (Fig. 6B), the basic histological structures are highly similar to that already described in *Scinax*. The pelvic girdle shows three cartilaginous areas corresponding to the presumptive pubis, ischium and ilium. At the centre of each element, hypertrophic chondrocytes are flanked by mature chondrocytes, surrounded by abundant ECM. Two masses of pre-muscular tissue are distinguishable, attached to the ischium and pubis. The masses are composed of highly elongated cells and their nuclei are visible. The dorsal mass is clearly composed of two presumptive muscles, which correspond to the pectineus and the iliacus internus. The ventral

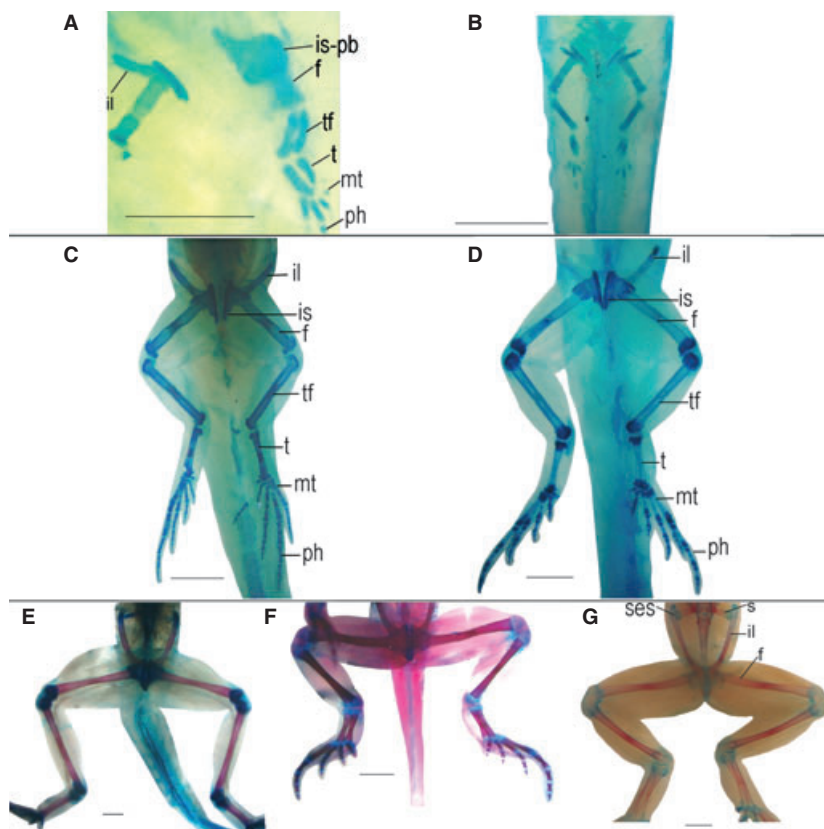


Fig. 5—*Pleurodema borellii*. Ventral view of the pelvic girdles and hind limbs of diaphanized specimens at different developmental stages. —**A**. Stage 35: The pelvic elements are separated; the segments of the hind limb are distinguishable, even little spots corresponding to the cartilaginous metatarsus and to the phalanx of Toe 4. —**B**. Stage 36: Note that the femurs are oriented to the posterior region of the body. —**C**. Stage 38: Note that the phalanges show the beginning of the ossification process in their central area. —**D**. Stage 41: The posterovenral surfaces of the pubis plate are in contact. —**E**. Stage 42: Note the pelvic girdle entirely closed and the complete ossification of the diaphyses of the long bones. —**F** and **G**. Stage 44 and 45: The sacral diapophyses are entirely ossified, and the sesamoid of each iliosacral joints are present. f, femur; il, ilium; is-pb, ischium–pubis; mt, metatarsus; ph, phalanx; ses, sesamoid of the iliosacral joint; t, tibiale; tf, tibiafibula. Scale bar: 1 mm.

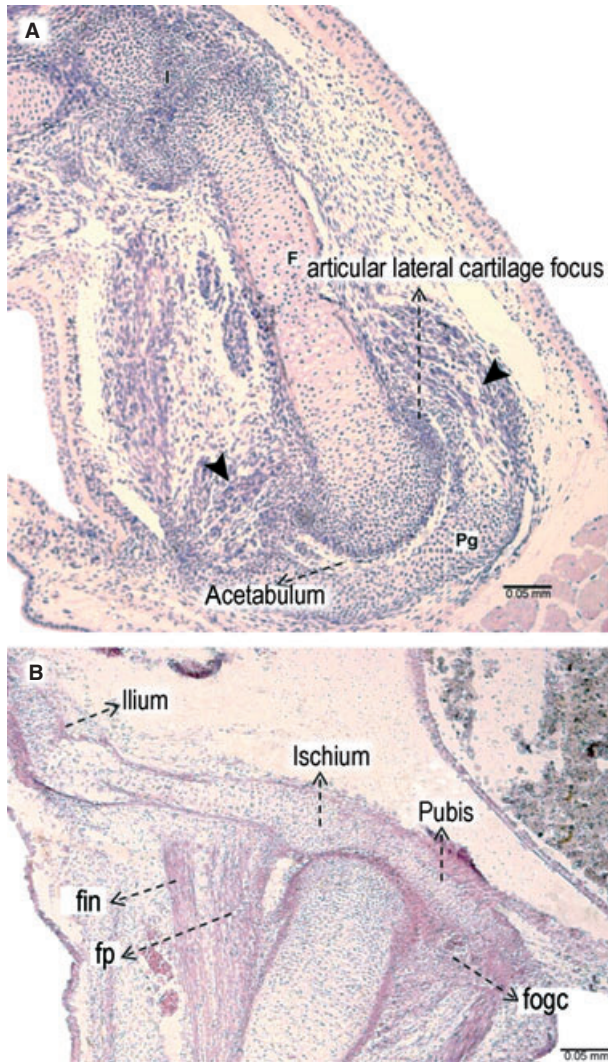


Fig. 6—**A.** Stage 35 of *Scinax squalirostris*. Histological section through hind limb and pelvic girdle. Continuous with the mesenchyme of the presumptive pelvic girdle, two zones of future muscular tissue are distinguishable (black arrowhead). The acetabulum is visible. The interzone remains in the area of the future joints of the femur with mesopodial segments. F, femur; I, interzone; Pg, pelvic girdle. —**B.** Stage 35 of *Pseudis minutus*. Histological section of the pelvic girdle. Two masses of future muscular tissue are distinguishable, attached to the ischium and pubis: the dorsal mass corresponds to the future pectineus and iliacus internus muscles, and the ventral mass corresponds to the anlagen of the gemelli–obturator complex. fin, future iliacus internus; fogc, future obturator gemellus complex; fp, future pectineus.

mass corresponds to the anlagen of the gemelli–obturator internus complex.

Pleurodema borellii Stage 36

The elements of the pelvic girdle are present forming a plate, with the pubis and ischium indistinguishable from each other

(Fig. 4B). The elements of the pelvic girdle are separated from each other (Fig. 5B). The ilium is posterior to the sacrum (Fig. 7A). The skeletal elements of the hind limbs are present and visible; the corresponding central area of each element presents perichondral ossification, except in the phalanges, which remain entirely cartilaginous. The femur is oriented to the posterior region of the body, as in the anterior stages (Fig. 5B). The hypochoord is completely ossified (Fig. 7A). In *L. latinasus*, the hypochoord is still cartilaginous (Fig. 7D); this element ossifies at Stage 41 (Fig. 7F). In *P. sawvagi*, the hypochoord is absent at this stage (Fig. 7G).

The histological data on *H. pulchellus* show that the pelvic girdle remains as a pre-chondrogenic focus, without differentiated elements (Fig. 8A). The femur is already cartilaginous, showing the reserve, proliferative and hypertrophic cell zones. The pre-myogenic masses begin to differentiate, elongating and orientating the cellular nuclei. At least seven pre-myogenic masses are already identifiable at the thigh (e.g. pectineus, adductor longus and adductor magnus muscles).

Pleurodema borellii Stage 37–38

The elements of the pelvic girdles remain separated (Fig. 5C). The ossification of the ilium has grown in the proximal direction (Fig. 4C), the rest of the girdle elements remain unchanged. The ilium rises to the level of the middle of the hypochoord and reaches the level of the first post-sacral element (Fig. 7B). The ilium starts to rotate to a horizontal position (Fig. 9B). The epiphyses of the long bones have the lateral articular cartilages clearly visible. The femur is oriented to the posterior region of the body (Figs 5C and 9A). The tarsal bones are present, and the phalanges begin to ossify at their diaphyses (Fig. 5C). In *P. sawvagi*, the ilium is still posterior to the first post-sacral element. In *H. riojanus*, the ilium is at the level of the anterior extreme of the hypochoord and the first post-sacral element.

The histological data on *P. borellii* (Fig. 8B) show that the pelvic girdle remains unchanged, as a pre-chondrogenic focus. The epiphyses of the long bones are clearly distinguishable and composed of pre-chondrogenic tissue. Adjacent to the lateral articular cartilage, the anlagen of a pre-tendon is observable. The femur shaft is composed of hyaline cartilage. The muscular-developing tissue exhibits large numbers of myofibrils. Most of the myofibrils are homogeneous, although some show striations. Many immature muscles, composed of fibres with big nuclei are clearly distinguishable, such as obturator internus, adductor magnus, gracilis major and minor and iliacus internus.

Pleurodema borellii Stage 39

No remarkable changes have been observed in relation to Stage 37–38. The ilium elongates in direction to the axial skeleton (Fig. 7C). In the case of *L. latinasus*, a second

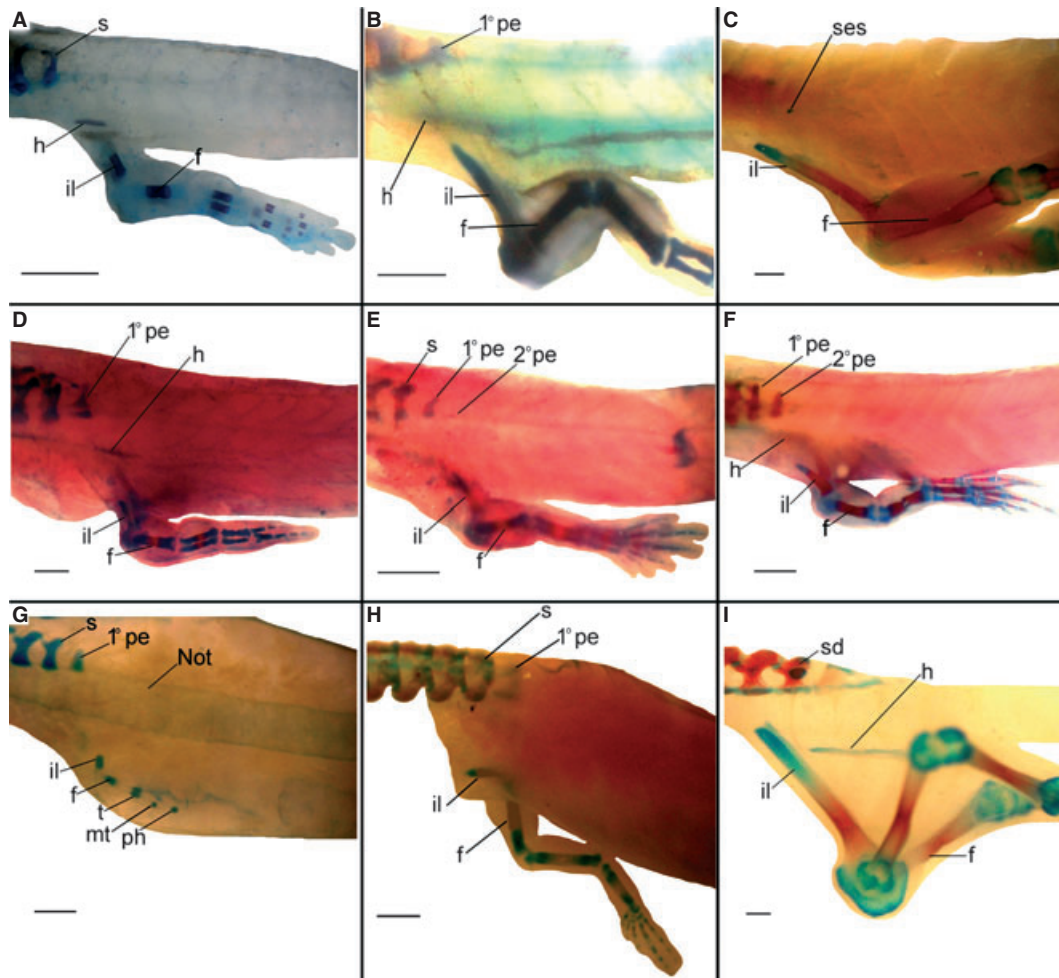


Fig. 7—Lateral view of different developmental stages of pelvic girdle and hind limb. —**A–C.** *Pleurodema borellii*. —**A.** Stage 36, note the ossified hypochord. —**B.** Stage 39. —**C.** Stage 41. —**D–E.** *Leptodactylus latinasus*. —**D.** Stage 36 note the hypochord still cartilaginous. —**E.** Stage 39, the ilium reaches the level of the second post-sacral element. —**F.** Stage 41. —**G–I.** *Phyllomedusa sauvagii*. —**G.** Stage 35, the hypochord is still absent. —**H.** Stage 39. —**I.** Stage 41. f, femur; h, hypochord; il, ilium; is-pb, ischium–pubis; mt, metatarsus; ph, phalanx; s, sacral vertebrae; sd, sacral diapophysis; ses, sesamoid of the iliosacral joint; t, tibiale; tf, tibiafibula; 1°pe, first post-sacral element; 2°pe, second post-sacral element. Scale bar, 1 mm.

post-sacral element is present, and the ilium reaches the level of this second element (Fig. 7E). In *P. sauvagii*, the ilium is at the level of the sacrum (Fig. 7H). In *P. azurea*, the hypochord is absent.

The histological data of *D. minutus* show that the ischium and pubis are cartilaginous, whereas the ilium is already composed of hypertrophied cells.

Pleurodema borellii Stage 40–41

Both elements of the girdle are in contact at the posteroventral surface of the pubis plate. The ossification of the ilium advances (Fig. 4D); this element almost reaches the level of the sacral diapophyses, anterior to the hypochord (Fig. 7C).

The ossification of the rest of the long bones is also well advanced. The femur is still oriented to the posterior region of the body. All bones increase in length (Fig. 5D). The sesamoids of the sacral diapophyses are distinguishable as small cartilaginous elements. In *P. sauvagii*, the anterior portion of each ilium passes the level of the sacral diapophyses, without touching them (Fig. 7I). In *P. azurea*, the ilium reaches the first post-sacral element. The second pair of post-sacral elements is present. The hypochord is already present and partially ossified. In *H. riojanus*, the ilium reaches the level of the sacral diapophyses, and the pelvic elements are entirely fused to each other, forming the girdle ring.

The histological data in *P. borellii* (Fig. 10B) show that the pelvic girdle consists of two cartilaginous elements

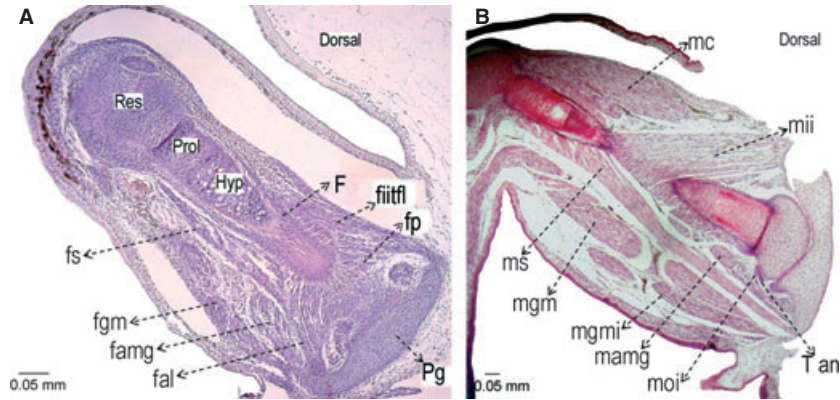


Fig. 8—**A.** Stage 36 of *Hypsiboas pulchellus*. Histological section of pelvic girdle and femur. The chondrogenic focus of the pelvic girdle is observable. The femur shows the reserve, proliferative and hypertrophic cartilaginous zones. Hyp, hypertrophic zone; Prol, proliferative zone; Res, reserve zone. —**B.** Stage 37 of *Pleurodema borellii*. Histological section showing the pelvic girdle, the femur shaft and many muscles masses clearly distinguishable. F, femur; fal, future adductor longus; famg, future adductor magnus; fgm, future gracilis major; fiitfl, future iliacus internus–tensor fasciae–latae; fp, future pectineus; fs, future semitendinosus; mamg; muscle adductor magnus; mc, muscle cruralis; mgm, muscle gracilis major; mgmi, muscle gracilis minor; mii, muscle iliacus internus; moi, muscle obturator internus; ms, muscle semitendinosus; Pg, pelvic girdle; T an, tendon anlage.

composed of mature chondrocytes. In these elements, only a crest in the pubis is morphologically differentiated, which corresponds to the floor of the acetabulum. From this stage, the half moon shape of each pelvic element is

restricted to the acetabulum. Meanwhile, the pre-acetabular iliac crest and the post-acetabular ischiadic crest grow forwards and backwards, respectively, forming a straight line, which allows the formation of a symphysis. The

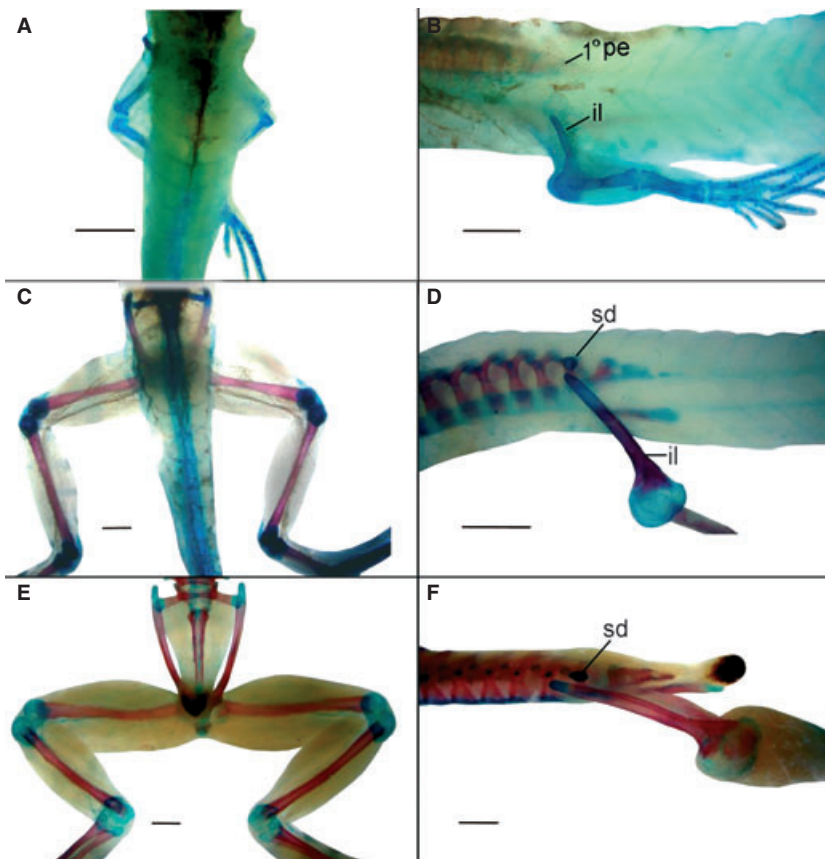


Fig. 9—*Pleurodema borellii*. Dorsal and lateral view of diaphanized specimens of Stages 38 (**A, B**), 42 (**C, D**) and 45 (**E, F**). Note the rotation of the ilium (**B, D**, and **F**) and the closer contact between the sacral diapophyses and the ilium (**D** and **F**). il, ilium; sd, sacral diapophysis; 1°pe, first post-sacral element. Scale bar: 1 mm.

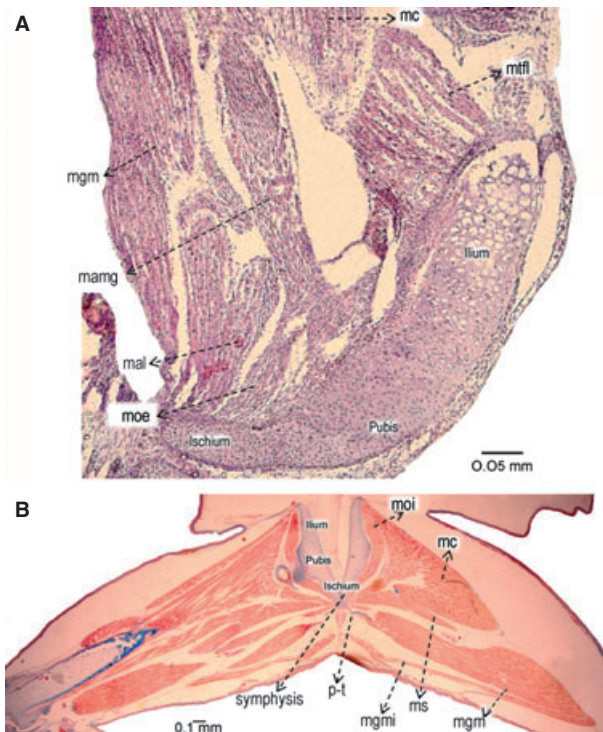


Fig. 10—**A.** Stage 39 of *Dendropsophus minutus*. Histological section through pelvic girdle showing the ischium and pubis cartilaginous, whereas the ilium is already composed of hypertrophied cells. The pre-muscular masses are differentiated. —**B.** Stage 41 of *Pleurodema borellii*. Histological section of pelvic girdle and thigh. The symphysis is already visible. The muscular masses are differentiated. mal, muscle adductor longus; mamg, muscle adductor magnus; mc, muscle cruralis; mgm, muscle gracilis major; mgmi, muscle gracilis minor; moe, muscle obturator externus; moi, muscle obturator internus; ms, muscle sartorius; mtf, muscle tensor faciae latae; p-t, pre-tendon.

pre-tendinous attachment of the gracilis major muscle to the pelvic girdle is observable.

Pleurodema borellii Stage 42

The pelvic elements are entirely fused to each other, forming the girdle ring (Fig. 5E). The ilium is almost completely ossified (4D). The ilium shaft forms an angle of 45° with respect to the horizontal plane. The sacral diapophyses and the ilium exhibit a closer contact, at the level of the anterior end of the ilium (Fig. 9D). The sacral diapophyses are enlarged but remain cartilaginous and immature. The long bones have finished the ossification process (Fig. 5E). The femur is oriented perpendicularly to the sagittal plane of the body (Figs 5E and 9C).

Pleurodema borellii Stage 43

The sacral diapophyses start to ossify at their proximal surfaces and remain articulated with the ilium extreme. A

remarkable difference between the terrestrial species and the arboreal *P. sauvagii* is the position of each ilium relative to the sacral diapophyses. In the latter species, the sacral diapophyses articulate at the level of the middle of the ilium. In *H. riojanus*, the proximal end of each ilium reaches the transverse process of the 8th pre-sacral vertebrae. The sacral diapophyses are expanded and ossified.

Pleurodema borellii Stage 44

The ischium starts to ossify. The iliac crest is visible (Fig. 4E).

Pleurodema borellii Stage 45

The ischium and the sacral diapophyses are almost entirely ossified (Fig. 4F). The sesamoid of each iliosacral joint is present. The ilium is almost in a horizontal plane, acquiring the normal adult position (Fig. 9F).

Pleurodema borellii Stage 46

The ilium reaches completely the horizontal position. In *P. sauvagii*, the ilium articulates with the sacral diapophysis, whereas in *P. azurea* it is still anterior to them (Fig. 11AB).

The histological data of Stage 42–45 on *P. borellii* (Fig. 12AB) show that the cartilaginous structures of each pelvic element are closely attached to each other. The femur shaft forms an acute angle with the sagittal plane of the body because the femur is elevated. The limb muscles are clearly formed.

The temporal sequences of the main events in the histogenesis of the muscle–skeletal tissues are presented in Table 1.

Character mapping

Fourteen characters that summarize the variability described above were selected for mapping on a phylogenetic tree (Fig. 13):

- (0) Ilium and sacral diapophyses are in contact at (i) late larval stages; (ii) early metamorphic stages and (iii) late metamorphic stages.
- (1) Ilium ossification begins at (i) early larval stages; (ii) late larval stages; (iii) early metamorphic stages and (iv) late metamorphic stages.
- (2) Ilium completes ossification at (i) late larval stages; (ii) early metamorphic stages and (iii) late metamorphic stages.
- (3) Ischium appears at (i) early larval stages and (ii) late metamorphic stages.
- (4) Medial surface of each ischium are in full contact to each other at (i) late larval stages; (ii) early metamorphic stages and (iii) late metamorphic stages.

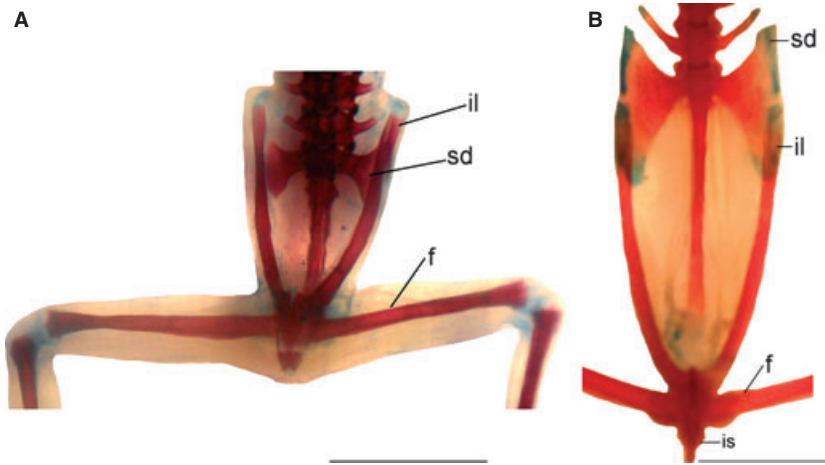


Fig. 11—*Phyllomedusa azurea*. —**A**. Stage 46, tip of the ilium is anterior to the sacral diapophysis; —**B**. Adult, the ilium articulates with the expanded sacral diapophysis. f, femur; il, ilium; is, ischium; sd, sacral diapophysis. Scale bar: 5 mm.

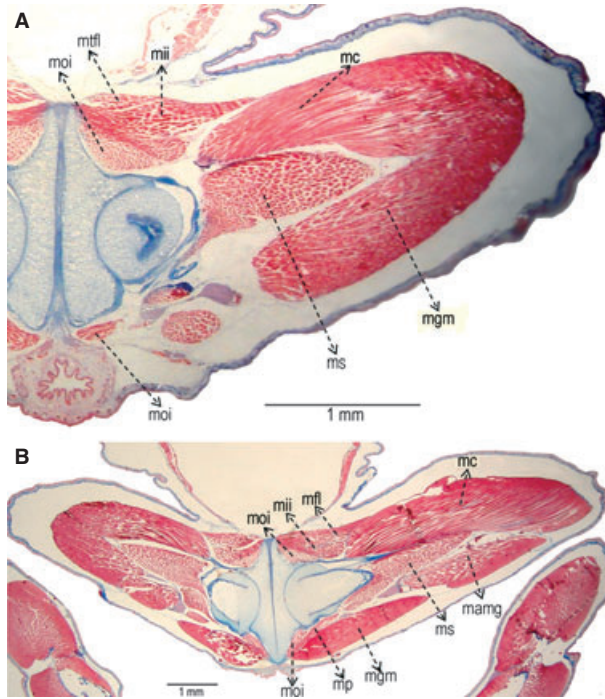


Fig. 12—**A**. Stage 42 of *Pleurodema borellii*. Histological section of pelvic girdle and thigh. Each pelvic element is closed and attached to each other. The limb muscles are clearly defined. m, muscle. —**B**. Stage 45 of *P. borellii*. Histological section of pelvic girdle and thigh, showing the limb muscles clearly formed. The femur shaft forms an acute angle to the sagittal plane of the body. mamg, muscle adductor magnus; mc, muscle cruralis; mii, muscle iliocostalis; mfl, muscle fasciae latae; mgm, muscle gracilis major; moi, muscle obturator internus; mp, muscle pectineus; ms, muscle sartorius; mtfl, muscle tensor fasciae latae.

- (5) Ischium ossification begins at (i) late larval stages; (ii) early metamorphic stages and (iii) late metamorphic stages.

- (6) Each pubis medial surface is in full contact with the other at (i) late larval stages; (ii) early metamorphic stages and (iii) late metamorphic stages.
- (7) The rotation of the iliac shaft reaches an angle of 45° at (i) late larval stages; (ii) early metamorphic stages and (iii) late metamorphic stages.
- (8) Sacral diapophyses appear at (i) early larval stages and (ii) late larval stages.
- (9) Sacral diapophyses begin to ossify at (i) late larval stages; (ii) early metamorphic stages and (iii) late metamorphic stages.
- (10) Hypochord appears at (i) early larval stages and (ii) late larval stages.
- (11) Hypochord fuses to the neural arches at (i) late larval stages; (ii) early metamorphic stages and (iii) late metamorphic stages.
- (12) Relationship between ilium and sacral diapophyses: (i) ilium shaft never exceeds the sacral diapophyses level and (ii) ilium shaft exceeds the sacral diapophyses level.
- (13) Adult shape of sacral diapophyses: (i) narrow. The distal extreme is slightly broader than the proximal one and (ii) expanded. The distal extreme is more than three times broader than the proximal one.

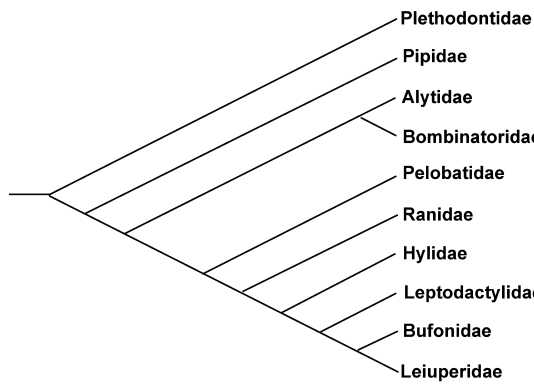
From those 14 characters, four support the monophyly of some group. Character 4, state a, supports the monophyly of Hyloides (Frost *et al.* 2006), with a reversion in Bufonidae (Fig. 14). Character 7, state a, also supports the monophyly of Hyloides. Character 12, state a, supports the monophyly of Acosmanura (Frost *et al.* 2006) (Fig. 14). Character 13, state a, supports the monophyly of Neobatrachia (Frost *et al.* 2006) (Fig. 14).

Discussion

Based on the analysis of cleared and stained specimens, Ročková and Roček (2005) described a pelvic girdle that developed from three early independent mesenchymatic elements that

Table 1 Comparison of the main events in the histogenesis processes of different taxa of anurans

Developmental events	Our data	Literature
Intrusion and division of ischiadic nerve	Stage 27–31 <i>Scinax squalirostris</i> and <i>Phyllomedusa sauvagii</i>	Stages 30–32 <i>Rana temporaria</i> (Pomikal <i>et al.</i> 2011); <i>Rana pipiens</i> (Dunlap 1967);
Mesenchymal condensation of femur and tibia–fibula	Stages 29–33 <i>S. squalirostris</i> and <i>P. sauvagii</i> <i>Hypsiboas pulchellus</i>	Stages 30–32 <i>R. temporaria</i> (Pomikal <i>et al.</i> 2011); <i>R. pipiens</i> (Dunlap 1967); <i>Xenopus laevis</i> (Newth 1956 in Dunlap 1967)
Four future muscular masses	Stage 33 <i>H. pulchellus</i>	Stage 31 <i>R. pipiens</i> (Dunlap 1967)
Massive split of future muscular mass	Stage 34 <i>S. squalirostris</i>	Stage 33–34 <i>R. pipiens</i> (Dunlap 1967)
Central areas of each presumptive long bone composed by mature hypertrophic chondrocytes	Stage 36–37 <i>Pleurodema borellii</i>	Stage 34 <i>R. pipiens</i> (Dunlap 1967); <i>X. laevis</i> (Newth 1956 in Dunlap 1967)
Muscles clearly defined in terms of position and ilium externally ossified and internally cartilaginous	Stage 41 <i>P. borellii</i>	Stage 36 <i>R. pipiens</i> (Dunlap 1967) Stage 41 <i>R. temporaria</i> (Pomikal <i>et al.</i> 2011)



Species	Locomotion	Habitat	0	1	2	3	4	5	6	7	8	9	10	11	12	13
<i>Xenopus laevis</i>	swimmer	aquatic	b	c	c	a	c	b	b	c	b	b	a	c	b	b
<i>Discoglossus pictus</i>	jumper/swimmer	aquatic/terrestrial	c	b	a,b	a	a,b,c	a,b,c	a,b,c	c	a,b	a,b,c	a	a,b,c	b	b
<i>Bombina bombina</i> <i>Bombina variegata</i>	swimmer	aquatic	a	b,c	c	a	c	c	b	b,c	a,b	a,b	a	c	b	b
<i>Pelobates fuscus</i>	Hopper-burrover	terrestrial	b,c	d	c	a	c	b,c	c	a	a	a	a	c	a	b
<i>Rana dalmatina</i>	jumper	terrestrial	a	b,c	c	a	c	c	c	c	a,b	b	a	c	b	a
<i>Phyllomedusa</i> <i>Hypsiboas andinus</i>	walker-jumper jumper	arboreal/terrestrial	a,b	a	b	a	a	b	a,b	a	a,b	a	b	c	b	b
<i>Leptodactylus latinasus</i>	jumper	terrestrial	a	?	?	?	a	?	?	a	b	?	a	?	a	a
<i>Bufo bufo</i>	crawling	terrestrial	a,b	b,c	c	b	a,b	c	b	c	b	a	a,b	c	a	a
<i>Pleurodema borellii</i>	jumper	aquatic/terrestrial	b	a	c	a	a	b	b	a	b	b	a	c	a	a

Fig. 13—Data matrix reduced to the family level. Character numbers and coding correspond to the list in the text.

can appear after the femur, tibia, fibula, astragalus and calcaneus are already formed (in *Discoglossus* and *Rana*), or synchronously with them (as in *Bombina*). Our histological data show that, at least in hylids, the pelvic girdle appears as early as Stage 31 in the ontogeny of most studied species, synchronously with the propodium and mesopodium. Shortly after its origin, the future pelvic girdle remains as a single mesenchymatic condensation until the skeletogenesis of the hind limbs is far advanced (see also Dunlap 1967; Pomikal *et al.* 2011). This pattern of formation of the pelvic girdle from one mesenchymatic condensation is also described for other vertebrates (Pomikal and Streicher 2010).

It has been currently interpreted that the anuran pelvic girdle arises from two chondrification centres (Green 1931; Ročková and Roček 2005). Our histological data show that after its origin, and inside the single mesenchymatic element

of the pelvic girdle, indeed, two chondrification centres do appear. These centres would correspond to the two chondrification centres described by Ročková and Roček (2005). Descriptions made in ranids (Ročková and Roček 2005; and Pomikal *et al.* 2011) show that the pattern of chondrification seems to be highly conserved. This chondrification process seems to start at the future iliac area, whereas the pubis is the last one to chondrify. However, our data show that the first chondrogenic centre that appears would correspond to the pubic precursor.

The emergence of the acetabulum occurs normally in tadpoles at the ontogenetic Stage 35, being the first of all the cavitation processes to appear. The second cavity, which corresponds to the knee, appears at Stages 38–39, suggesting a proximo-distal sequence in the formation of the joints between pelvic girdle and hind limb, and the intrinsic

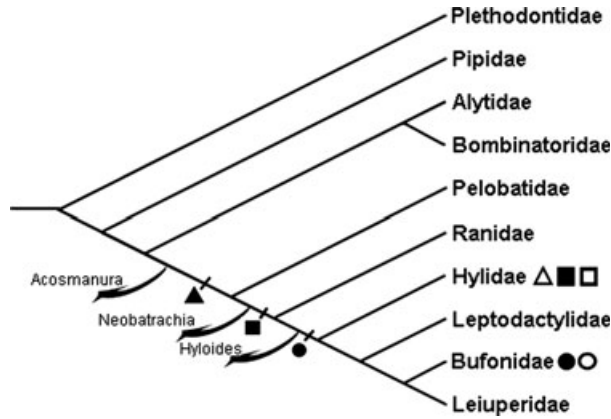


Fig. 14—Phylogenetic mapping of characters 4 (full contact of medial surfaces of ischium), 12 (relationship between ilium and sacral diapophyses) and 13 (adult shape of sacral diapophyses) on the amphibian phylogenetic hypothesis of Frost *et al.* (2006), with the modifications proposed by Grant *et al.* (2006), reduced to family level. Solid circle: character 4, state a (late larval stages); empty circle: state b (early metamorph stages). Solid triangle: character 12, state a (ilium shaft never exceed the sacral diapophyses level); empty triangle: state b (ilium shaft exceed the sacral diapophyses level). Solid square: character 13, state a (narrow); empty square: state b (expanded).

elements of the hind limb. Interestingly, the acetabulum appears before the muscles are mature (see results and Fig. 15). This is a noteworthy sequence because it has been frequently stressed that the contraction of the muscles is fundamental in maintaining joint progenitors committed to their fate, a requirement for correct joint cavitation and morphogenesis (Pitsillides 2006; Kahn *et al.* 2009). Knee cavitation occurs after all skeletal tissues, cartilage, muscles and tendons are formed (see results and Fig. 15). Incongruence in the response of the joints to the movement caused by early muscular contractions has been previously documented (Kahn *et al.* 2009; Abdala and Ponssa 2012). Probably in some joints, the delayed development of the musculature was compensated by other components in the genetic programme that regulates joint development (Kahn *et al.* 2009). Another possible explanation is that the response of mesenchymal stem

cells in the embryonic limb to the biophysical stimuli may depend upon the location of the cells. This suggests that a complex interaction would exist between mechanical forces and location-specific regulatory factors, affecting bone and joint development (Nowland *et al.* 2010).

The rotation of the femur from a posterior to an anterior location, the rotation of the ilium to a horizontal position and the approach of each pelvic element, which are normal events during anuran ontogeny, are probably related to the transition from a motile stage to the fully functional stage of Muntz (1975). Each femur, ilium and pelvic elements require mature muscles capable of maintaining the elements in their normal position. At the end of the fully functional stage (Muntz 1975), the femur is in the right position to perform the saltatory locomotion, that is, completely rotated to an anterior location. It is only at this stage that the muscle exhibits the phenotype of completely mature fibres: elongated, striated, with no visible nuclei, and therefore capable of sustaining the skeletal structures in their normal position.

Our data indicate that ilium elongation is a process that occurs between Stages 35 and 46; this is in agreement with data provided by Pomikal *et al.* (2011), who stated that ilium elongation in *R. temporaria* occurs between Stages 35 and 41. Elongation of the ilium has been repetitively associated with jumping abilities in frogs (Gans and Parsons 1966; Prikryl *et al.* 2009). Pomikal and Streicher (2010) described a similar process in *Mus musculus*, indicating that the main function of ilium elongation is probably related to the establishment of the ilio-sacral joint. It could be hypothesized that although in tetrapods ilium elongation arises to link the axial skeleton and the pelvic girdle, an allometric process involving a remarkable expansion of the ilium and urostyle occurred in frogs and allowed the jumping locomotion.

Comparing our data with those of other tetrapod taxa (Malashichev 2001; Malashichev *et al.* 2008; Pomikal and Streicher 2010), it can be observed that at least two events of the pelvic girdle development are conserved across all those taxa: 1) There is only one mesenchymatic condensation involved in the origin of the pelvic girdle (Malashichev 2001; Malashichev *et al.* 2008; Pomikal and Streicher 2010; Pomikal *et al.* 2011; this work). 2) The pelvic girdle chondrifies

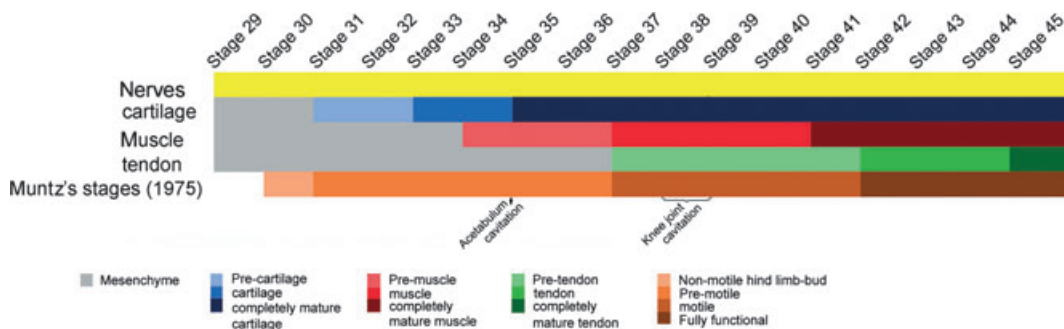


Fig. 15—Tissue differentiation sequence based on the present histological data.



Fig. 16—Pelvic girdle of *Pleurodema borellii* Stage 42 showing the muscles with the tendon surrounding the acetabulum joint.

relatively late during embryogenesis after the beginning of chondrification in the hind limb (Malashichev 2001; Malashichev *et al.* 2005, 2008; Pomikal and Streicher 2010; Pomikal *et al.* 2011).

The sequences of tissue differentiation demonstrated by our data are similar to those findings reported by Dunlap (1967) and Muntz (1975). If all these data are considered together, the sample includes taxa widely dispersed on the phylogenetic anuran tree (e.g. Frost *et al.* 2006). Thus, it may be inferred that processes of tissue differentiation in the limb bud would be highly conserved among anurans. In fact, our Table 1 shows that the variation in the timing of emergence of the main histological events never exceeds two stages. Variability in the timing of the organization of the gross anatomy seems to be more plastic than the highly conserved tissue differentiation. According to our data, the following sequence of the limb bud tissue differentiation can be proposed: (i) cartilage, (ii) muscles and (iii) tendons (Fig. 15). Comparing with other vertebrates, this sequence is apparently not congruent with the molecular data gathered, for example, in birds by Kardon (1998). The author showed that tenascin is the first identifiable ECM component. Thus, according to her data, tendon precursors are the first in appearing inside the limb bud. After that, the muscle patterning begins with the migration and aggregation of myoblasts into the dorsal and ventral region of the limb bud (Kardon 1998). It should be considered, however, that the ECM with the tenascin is related to the tendinous primordia that in fact are mesenchymatic cells. Hence, phenotypically, those cells are not really tendon yet. Our sequence is proposed based on cell differentiation that can be seen as an emergent property of the molecular differentiation. In fact, it should be considered that Kardon's (1998) data on cell differentiation are in agreement with our findings.

As can be seen in Fig. 15, the processes of tissue differentiation are not synchronic (i.e. differentiation of the muscular

tissue as such begins once the cartilaginous tissue is clearly recognizable). Muntz (1975) proposed four stages in limb development relating the muscular maturity and movement possibilities: non-motile stage, pre-motile stage, motile stage and fully functional stage. Our data show that the intrusion of the ischiadic nerve into the limb bud is produced very early in the tadpole ontogeny. Pre-chondrogenic condensation appears at Stage 31, which corresponds to a pre-motile stage of Muntz (1975), the stage at which the limb is directly excitable by electrical stimulation of a spinal nerve. We suggest that the nerve would be producing a movement analogous to the 'embryonic motility' (Müller 2003) that would induce the emergence of the pre-cartilage. Cartilage is the only tissue that reaches maturity before the limb is motile. The cartilaginous structures have a pioneer role in determining a topographical differentiation inside the limb bud. This topographical arrangement, plus the location of the tendon primordia as described by Kardon (1998), probably collaborates in organizing the position of the muscular complexes. However, it is just at the beginning of the motile stage that the muscular differentiation, pre-tendon emergence and connection between them and the cartilages occur. Despite the presence of the nerves since the beginning of the tadpole ontogeny (Stage 26), the movement is not possible because the structures that should be moved are not formed yet. Indeed, it seems that in anurans, embryonic motility also closes the spinal circuitry, as was shown in chicken embryos (Bradley 1999). Probably, the early emergence of the movement acts as a feed-back stimulus that drives the posterior total differentiation of the tissues involved (fully functional stage in Muntz 1975). Only at the motile stage, do the muscles reach complete maturity. By contrast, the tendon is the only tissue that requires a fully functional member to be mature (Fig. 16). Kardon (1998) also stressed that after their formation, tendon primordia need an interaction with muscle for their maintenance and subsequent segregation into individual tendons. In the absence of muscles, the tendon primordia degenerate.

According to Schweitzer *et al.* (2010), several mechanisms could underlie the accurate connectivity, through tendons, between cartilage, muscles and bones. Our data support their first proposed mechanisms, in which a parallel independent development of each tissue involved is followed by the induction of connectivity between these tissues, such as muscle–cartilage connection. Movement seems to be a main eliciting factor to induce this connectivity. However, the developmental events follow a sequential pattern. Once the cartilaginous elements and muscles are almost completely differentiated, the tendon anlage is recognizable. All these events occur at the motile stage (Muntz 1975); muscles and cartilaginous elements appear before the connexions between them are formed. Kardon (1998) mentioned that in chick embryos, developing muscle and tendon may be closely associated as early as Stage 25–26, but mature myotendinous junctions do not begin to form until Stage 34 (Tidball and Lin 1989; Kardon 1998). Our data indicate that tendon differentiation is

produced once the muscular masses are formed, which is in agreement with Schweitzer *et al.* (2010), who stressed that signals from the muscles are essential for tendon differentiation at subsequent stages (Schweitzer *et al.* 2010).

Muscular differentiation seems to be an extremely fast morphological process compared to the differentiation of the limb skeletal element, which can be interpreted as an exceptionally precise and sequential model of divisions and branching (Shubin and Alberch 1986; Fabrezi and Alberch 1996; Fabrezi *et al.* 2007). At only one stage (e.g. from Stages 33 to 34), a transition from 2 to 11 muscular masses occurs. Dunlap (1967) reported a slight post-axial dominance in relation to the hind limb muscle differentiation in *R. pipiens*, and our data revealed a proximo-distal gradient of differentiation. We discern a proximo-distal gradient of differentiation in relation to the size of the pre-myogenic complexes, the proximal being larger than the distal ones. Moreover, our data suggest an explosive and simultaneous differentiation of all 11 muscular masses together (see also Kardon 1998; Fig. 5). Once again, the general process of hind limb muscle morphogenesis seems to be highly conserved in tetrapods.

Character mapping

All adult anurans have an articulation between the anterior extreme of the ilium and the sacral diapophyses, named ilio-sacral articulation or joint. However, in several frog species, this joint is formed only at the final developmental stages; at earlier stages, the tips of their iliac shafts reach far beyond the anterior margin of the expanded sacral diapophyses and then return to their final position. These changes of the ilium position with respect to the sacral diapophyses are observed in arboreal frogs, such as *P. sauvagii*, *P. azurea* and *H. riojanus*, and were also reported by Ročková and Roček (2005) for aquatic anurans, such as *Xenopus* and *Bombina*. According to the present character mapping, the iliac shaft that never exceeds the sacral diapophyses level is a synapomorphy at the Acosmanura level, with a reversion in Hylidae (Frost *et al.* 2006). Therefore, this character is homoplastic in Hylidae and could be related to ecophysiological requirements in the tadpole life. Hylids are also quite different from the remaining members of the Hyloides in other characters. They present an early ossification of the ilium and a delayed emergence of the hypochord. Interestingly, all these characters are visible only during development, because in adults, they show the same configuration of the rest of anurans.

According to our data, sacral diapophyses are expanded in the adult hylids (character 13); however, Pugener and Maglia (2009) reported narrow sacral diapophyses in *Acris crepitans*. We coded our character 13 considering their data and obtained a synapomorphy for Neobatrachia. Most of our selected characters that have been traditionally considered to be very adaptive (e.g. adult shape of sacral diapophyses; full contact of ischium medial surface) are synapomorphies. Simons (2008) also found that many char-

acters of the pelvic girdle that were considered adaptive (Emerson 1982) have no significant relationship with locomotor style (e.g. pelvic length, urostyle length). In addition, the characters we analysed show variations in the timing of some developmental processes, highlighting the importance of the heterochrony as a main factor driving morphological differentiation in anurans.

Conclusions

Our data evidence that there is just one mesenchymal condensation involved in the origin of the pelvic girdle in Anura. The pelvic girdle arises from two centres of chondrification, the pubic precursor being the first to emerge. The acetabulum is the first cavitation event to occur and it does so before the muscles are mature. The knee cavitation starts after all skeletal and muscular tissues are formed. The sequence of tissue differentiation in anura is highly conserved: (i) cartilage; (ii) muscles and (iii) tendons. Most of the differences found in the taxa studied are related to the gross anatomy of the analysed structures, the timing of the histogenesis being highly conserved. Muscular differentiation seems to be a fast morphological process. There are variations in the order of the differentiation of the elements of pelvic girdle in the hylid species analysed, showing heterochronic events driving the differentiation of these elements in frogs.

Acknowledgements

We are grateful to Sirisha Herat for reading our manuscript. Grant sponsor: CONICET; Grant number: PIP 112-200801-00225. Grant sponsor: FONCYT; Grant numbers: PICT 12418-06-223; PICT 2008-0578.

References

- Abdala, V. and Ponssa, M. L. 2012. Life in the slow lane: The effect of reduced mobility on tadpole limb development. – *The Anatomical Record* **295**: 5–17.
- Bancroft, J. D. and Gamble, M. 2002. Theory and Practice of Histological Techniques, pp. 200. Churchill Livingstone Press, Edinburgh.
- Bradley, N. S. 1999. Transformations in embryonic motility in chick: Kinematic Correlates of Type I and II Motility at E9 and E12. – *Journal of Neurophysiology* **81**: 1486–1494.
- Buckingham, M., Bajard, L., Chang, T., Daubas, P., Hadchouel, J., Meilhac, S., Montarras, D., Rocancourt, D. and Relaix, F. 2003. The formation of skeletal muscle: From somite to limb. – *Journal of Anatomy* **202**: 59–68.
- Chanoine, C. and Hardy, S. 2003. *Xenopus* muscle development: From primary to secondary myogenesis. – *Developmental dynamics* **226**: 12–23.
- Duellman, W. E. and Trueb, L. 1986. Biology of Amphibians. The John Hopkins University Press, Baltimore, MD.
- Dunlap, D. G. 1967. The development of the musculature of the hindlimb in the frog, *Rana pipiens*. – *Journal of Morphology* **119**: 241–258.
- Ecker, A. 1889. The Anatomy of the Frog. Clarendon Press, Oxford.

- Emerson, S. 1979. The iliosacral articulation in frogs: Form and function. – *Biological Journal of the Linnean Society* **11**: 153–168.
- Emerson, S. 1982. Frog poscranial morphology: Identification of a functional complex. – *Copeia* **1982**: 603–613.
- Fabrezi, M. 1993. The anuran tarsus. – *Alytes* **11**: 47–63.
- Fabrezi, M. and Alberch, P. 1996. The carpal elements of anurans. – *Herpetologica* **52**: 188–204.
- Fabrezi, M. and Barg, M. 2001. Patterns of carpal development among anuran amphibians. – *Journal of Morphology* **249**: 210–220.
- Fabrezi, M., Abdala, V. and Martínez Oliver, I. 2007. Developmental basis of limb homology in lizards. – *Anatomical Record* **290**: 900–912.
- Felisbino, S. L. and Carvalho, H. F. 1999. The epiphyseal cartilage and growth of long bones in *Rana catesbeiana*. – *Tissue Cell* **31**: 301–307.
- Frost, D. R., Grant, T., Faivovich, J., Bain, R. H., Haas, A., Haddad, C. F. B., et al. 2006. The amphibian tree of life. – *Bulletin of the American Museum of Natural History* **297**: 1–370.
- Gans, C. and Parsons, T. S. 1966. On the origin of the jumping mechanism in frogs. – *Evolution* **20**: 92–99.
- Goloboff, P., Farris, J. and Nixon, K. 2003. T.N.T.: Tree analysis using new technology. Program and documentation available from the authors. www.zmuc.dk/public/phylogeny (accessed 13 March 2011).
- Gosner, K. L. 1960. A simplified table for staging anurans embryos and larvae with notes on identification. – *Herpetologica* **16**: 183–190.
- Grant, T., Frost, D. R., Caldwell, J. P., Gagliardo, R., Haddad, C. F. B., Kok, P. J. R., Means, D. B., Noonan, B. P., Schargel, W. E. and Wheeler, W. C. 2006. Phylogenetic systematics of dart-poison frogs and their relatives (Amphibia: Athesphatanura: Dendrobatidae). – *Bulletin of the American Museum of Natural History* **229**: 262.
- Green, T. L. 1931. On the pelvis of the anura: A study in adaptation and recapitulation. – *Proceeding of the Zoological Society of London* **1931**: 1259–1289.
- Jenkins, F. A. and Shubin, N. H. 1998. *Prosalirus bitis* and the anuran caudopelvic mechanism. – *Journal of Vertebrate Paleontology* **18**: 495–510.
- Kahn, J., Shwartz, Y., Blitz, E., Krief, S., Sharir, A., Breitel, D. A., et al. 2009. Muscle contraction is necessary to maintain joint progenitor cell fate. – *Developmental Cell* **16**: 734–743.
- Kardon, G. 1998. Muscle and tendon morphogenesis in the avian hind limb. – *Development* **125**: 4019–4032.
- Maglia, A. M., Pugener, L. A. and Mueller, J. M. 2007. Skeletal morphology and postmetamorphic ontogeny of *Acris crepitans* (Anura: Hylidae): A case of miniaturization in frogs. – *Journal of Morphology* **268**: 194–223.
- Malashichev, Y. B. 2001. Sacrum and pelvic girdle development in lacertidae. – *Russian Journal of Herpetology* **8**: 1–16.
- Malashichev, Y. B., Borkhvardt, V. G., Christ, B. and Scaal, M. 2005. Differential regulation of avian pelvic girdle by the limb field ectoderm. – *Anatomy and Embryology* **210**: 187–197.
- Malashichev, Y., Christ, B. and Pröls, F. 2008. Avian pelvis originates from lateral plate mesoderm and its development requires signals from both ectoderm and paraxial mesoderm. – *Cell and Tissue Research* **331**: 595–604.
- Manzano, A. S. 1996. Análisis de la musculatura de la familia Pseudidae (Amphibia: Anura). PhD Thesis. Universidad Nacional de Tucumán, Tucumán.
- Manzano, A. S. and Barg, M. 2005. The iliosacral articulation in Pseudinae (Anura: Hylidae). – *Herpetologica* **61**: 259–267.
- Müller, G. 2003. Embryonic motility: Environmental influence and evolutionary innovation. – *Evolution and Development* **5**: 56–60.
- Muntz, L. 1975. Myogenesis in the trunk and leg during development of the tadpole of *Xenopus laevis* (Daudin 1802). – *Journal of Embryology and Experimental Morphology* **33**: 757–774.
- Newth, D. R. 1956. On the neural crest of the lamprey embryo. – *Journal of Embryology and Experimental Morphology* **4**: 358–375.
- Nixon, K. C. 1999. Winclada (BETA) ver. 0.9.9. published by the author, Ithaca, NY.
- Nowland, N. C., Bourdon, C., Dumas, G., Tajbakhsh, S., Prendergast, P. and Murphy, P. 2010. Developing bones are differentially affected by compromised skeletal muscle formation. – *Bone* **46**: 1275–1285.
- Pitsillides, A. 2006. Early effects of embryonic movement: “A shot out of the dark”. – *Journal of Anatomy* **208**: 417–431.
- Pomikal, C. and Streicher, J. 2010. 4D-Analysis of early pelvic girdle development in the mouse (*Mus musculus*). – *Journal of Morphology* **271**: 116–126.
- Pomikal, C., Blumer, R. and Streicher, J. 2011. Four-dimensional analysis of early pelvic girdle development in *Rana temporaria*. – *Journal of Morphology* **272**: 287–301.
- Ponssa, M. L., Goldberg, J. and Abdala, V. 2010. Sesamoids in anurans: New data, old issues. – *Anatomical Record* **293**: 1646–1668.
- Přikryl, T., Aerts, P., Havelková, P., Herrel, A. and Roček, Z. 2009. Pelvic and thigh musculature in frogs (Anura) and origin of anuran jumping locomotion. – *Journal of Anatomy* **214**: 100–139.
- Pugener, L. A. and Maglia, A. M. 2009. Developmental evolution of the anuran sacro-urostylic complex. – *South American Journal of Herpetology* **4**: 193–209.
- Reilly, S. M. and Jørgensen, M. E. 2011. The evolution of jumping in frogs: morphological evidence for the basal anuran locomotor condition and the radiation of locomotor systems in crown group anurans. – *Journal of Morphology* **272**: 149–168.
- Ročková, H. and Roček, R. 2005. Development of the pelvis and posterior part of the vertebral column in the anura. – *Journal of Anatomy* **206**: 17–35.
- Schweitzer, R., Zelzer, E. and Volk, T. 2010. Connecting muscles to tendons: Tendons and musculoskeletal development in flies and vertebrates. – *Development* **137**: 2807–2817.
- Shubin, N. H. and Alberch, P. 1986. A morphogenetic approach to the origin and basic organization of the tetrapod limb. – *Evolutionary Biology* **20**: 319–387.
- Simons, V. F. H. 2008. Morphological correlates of locomotion in anurans: limb length, pelvic anatomy and contact structures. Thesis. College of Arts and Sciences of Ohio University, Athens, OH.
- Smetanick, M., de Sá, R. O. and Radice, G. P. 2000. Do timing and pattern of myogenesis correlate with the life history mode in anurans? – *Journal of Herpetology* **34**: 637–642.
- Tidball, J. G. and Lin, C. 1989. Structural changes at the myogenic cell surface during the formation of myotendinous junctions. – *Cell and Tissue Research* **257**: 77–84.
- Totty, B. A. 2002. Mucins. In: Bancroft, J. D. and Gamble, M. (Eds): *Theory and Practice of Histological Techniques*, pp. 163–200. Churchill Livingstone Press, New York.
- Trueb, L. 1973. Bones, frogs and evolution. In: Vial, J. L. (Ed.): *Evolutionary Biology of the Anurans; Contemporary Research on Major Problems*, pp. 65–132. The University Missouri Press, Columbia.
- Trueb, L., Pugener, L. A. and Maglia, A. M. 2000. Ontogeny of the bizarre: An osteological description of *Pipa pipa* (Anura: Pipidae), with an account of skeletal development in the species. – *Journal of Morphology* **243**: 75–104.
- Wassersug, R. J. 1976. A procedure for differential staining of cartilage and bone in whole formalin-fixed vertebrates. – *Staining Techniques* **51**: 131–134.

Appendix 1

	Stage	Specimen number	
<i>Hypsiboas riojanus</i>	39–40	FML16595 (diaphanized)	
	41	FML16595 (diaphanized)	
	43	FML16637 (diaphanized)	
	45	FML165595 (diaphanized)	
<i>Hypsiboas pulchellus</i>	33	DIAML009 (histological)	
<i>Phyllomedusa azurea</i>	39	UNNEC7409 (diaphanized)	
	40	UNNEC7409 (diaphanized)	
	41	UNNEC7409 (diaphanized)	
	46	UNNEC7409 (diaphanized)	
<i>Phyllomedusa sauvagii</i>	30	DIAM L 016 (histological)	
	31	DIAM L 016 (histological)	
	36	MCN57 (diaphanized)	
	37	MCN57 (diaphanized)	
	38	MCN57 (diaphanized)	
	39	MCN57 (diaphanized)	
	40	MCN57 (diaphanized)	
	41	MCN57 (diaphanized)	
	42	L920 (diaphanized)	
	46	L920 (diaphanized)	
	Adult	MCN258 (diaphanized); FML03822–823 (diaphanized)	
	<i>Scinax squelirostris</i>	26	DIAM004 (histological)
		27	DIAM004 (histological)
28		DIAM004 (histological)	
29		DIAM004 (histological)	
30		DIAM004 (histological)	
34		DIAM004 (histological)	
35	DIAM004 (histological)		
<i>Dendropsophus minutus</i>	39	DIAM L005 (histological)	
<i>Pseudis minutus</i>	35	DIAM020 (histological)	
<i>Leptodactylus latinasus</i>	36	FML 24565 (diaphanized); FML 24592 (diaphanized)	
	37	FML 24583 (diaphanized); FML 24591	
	38	FML 24584 (diaphanized); FML 24586–587	
	39	FML 24581–582 (diaphanized);	
	40	FML 24567–580 (diaphanized); FML 24585 (diaphanized);	
	41	FML 24588–590 (diaphanized)	
	42	FML 24566 (diaphanized)	

Appendix 1 (continued)

	Stage	Specimen number
<i>Pleurodema borellii</i>	26–32	FML 24733 (diaphanized)
	29	FML 24552–553 (diaphanized)
	32	FML 24548 (diaphanized); FML 24550–551 (diaphanized); FML 24556 (diaphanized)
	33	FML 24546 (diaphanized); FML 24561–562 (diaphanized)
	34	FML 24541–24545 (diaphanized); FML 24547 (diaphanized)
	35	FML 24549 (diaphanized); FML 24557 (diaphanized); FML 24559–560 (diaphanized);
	36	FML 24563 (diaphanized)
	37	FML 24514 (diaphanized); FML 24517 (diaphanized); FML 24539–540 (diaphanized);
	38	FML 24554–555 (diaphanized); FML 24564 (diaphanized)
	39	FML 24522 (diaphanized); FML 24537 (diaphanized); FML 24558 (diaphanized)
	41	L918, (histological); FM24538
	42	FML 24687 (histological); FML 245533 (diaphanized)
	43	FML 245819 (diaphanized); FML 24518 (diaphanized); FML 24520 (diaphanized);
	44	FML 24529–530 (diaphanized)
	45	FML 24521 (diaphanized); FML 24531–532 (diaphanized); FML 24534–535 (diaphanized)
		FML 24519 (diaphanized); FML24524 (diaphanized); FML 24536 (diaphanized)
		FML 24527 (diaphanized)
	FML 24690 (histological); FML 24515–516 (diaphanized); FML 24523 (diaphanized); FML 24525 (diaphanized); FML 24528 (diaphanized)	
	FML 24526 (diaphanized)	
	FML 24690 (histological)	

FML, Fundación Miguel Lillo collection; DIAM-L: CCyTTP- CONICET amphibian larval collection, Diamante, Entre Ríos, Argentina; L: private collection of María Laura Ponssa; MCN: Museo de Ciencias Naturales de la Universidad Nacional de Salta collection, Salta, Argentina; UNNEC: Universidad Nacional del Nordeste collection, Corrientes, Argentina.